SHEET ELECTROMAGNETIC FORMING USING CONVEX PUNCH INSTEAD OF CONCAVE DIE

E. Eshghi and M. Kadkhodayan*

* *kadkhoda@um.ac.ir*

Received: March 2015 **Accepted: October 2015**

Department of Mechanical Engineering, Ferdowsi University of Mashhad, Mashhad, Iran.

Abstract: *High speed and absence of a precise control over pressure distribution confine sheet Electromagnetic Forming into a die to simple shapes having shallow depth. It is possible to reach a higher depth by using a convex punch instead of a concave die. In this study, sheet Electromagnetic Forming on a punch and sheet Electromagnetic Forming into a die are investigated. The electromagnetic part of the study is investigated analytically and its mechanical part is studied numerically. In order to couple electromagnetic with mechanical parts, no-coupling method is used. The obtained results are verified by comparing the obtained results with previous experimental ones in literature. Rate-dependent and rate-independent hardenings are taken into consideration for the mechanical behavior for material of AAl1050. Using appropriate hardening model for material yields acceptable results. Moreover, a convex punch instead of a concave die is used to reach to a higher depth in sheet Electromagnetic Forming.*

Keywords: *High speed forming, Electromagnetic forming, Convex punch, FEM, Strain rate.*

1. INTRODUCTION

Mechanical behavior of materials under dynamic loading compared with quasi-static conditions can vary considerably. The material changing behavior has advantages such as reducing spring-back and forming improvement. Studying and industrializing high speed forming techniques which can be the subject of most of the researches on forming metals.

Electromagnetic forming (EMF) process is a high speed forming process which has its roots in producing Lorentz forces created by a magnetic field. The magnetic field causes eddy current on workpiece. These eddy currents generate secondary magnetic field. The workpiece is driven away from coil because of the mutual interaction between the secondary and primary magnetic fields. The repulsive force is large enough to exert a tension greater than the yield strength of material and cause permanent deformation of the workpiece.

Electromagnetic forming process is divided into two main groups, circular components forming and flat sheets forming. Most studies have been on circular components forming shape and fewer is devoted to flat sheets forming; hence, it can be studied here for further research in this area. Kapitza [1] 1924 was the first person who used electromagnetic forces to form conductive materials in 1958, Harvey and Brower [2] for the first time had experimental studies in the field of electromagnetic products to compress and expand the shape of metals. Gobl [3] stated that it is impossible to have a closed-form analytical solution for electromagnetic sheet forming because of the workpiece deformation. Al-hassani [4] suggested an approximate analytical solution for calculating the magnetic pressure of a coil designed by him. Takatsu [5] used a flat spiral coil to free-form sheets and the experimental results were consistent with their numerical solutions. Risch [6] investigated sheet free forming and some changes of parameters such as battery energy and coil geometry on formability quality experimentally and numerically. They concluded that EMF with die is more complicated and difficult in comparison to free forming. Oliveira et al. [7] conducted numerical simulation and experimental study to form aluminum alloys AA5182 and AA5754 and free forming and forming into a die were investigated. Neugebauer [8] investigated the field of EMF sheet experimentally. Aluminum alloy AA5182 was formed into a cube mold and the results were compared with changes in the charge energy. They also showed that if vacuum was not

[DOI: 10.22068/ijmse.13.2.1]

provided properly, the trapped air prevent from proper forming. Xu et al. [10] presented a reasonable approximate solution to determine the magnetic pressure distribution on the sheet in the electromagnetic sheet forming process. Xiao et al. [11] simulated a three-dimensional electromagnetic sheet forming with a strong coupling method. They compared the results obtained from the numerical simulation with the experimental results of Takatsu and Partners [5].

Having a review on the literature, one can simply observe that most studies in this area are devoted to forming without a die and a few are dealt with forming with a die. Sheet electromagnetic forming of sheet has been confined to simple shapes with shallow depth, therefore gaining a greater depth in forming could be one of the main goals of future research [8]. This study aims to gain a greater depth in the workpiece by applying a convex punch rather than the common forming technique using a concave die. The process is divided into two sections, i.e. electromagnetic and mechanical. The coupling method is used for the solution procedure. The electromagnetic and forming parts are investigated analytically and numerically, respectively. The experimental data given by Takatsu [5] are used to verify the results and the same material of AAl1050 is used. The strain-rate-independent dependent models are applied to observe the hardening behavior of material and the obtained results are compared to each other. After verifying the solution, the electromagnetic forming on punch and forming sheet into a die are studied. Because of different boundary conditions of the electromagnetic forming new coils are designed.

2. THE ELECTROMAGNETIC PART OF THE PROCESS

In non-coupling method in order to calculate the magnetic pressure on the sheet, the work piece deformation is avoided. Magnetic pressure producing by the coil is obtained by the following equation [6]

$$p(r,t)=\frac{\mu_\circ}{2}B^2(r,t) \qquad (1)$$

in which p is magnetic pressure, $\mu_\circ$ is the coefficient of magnetic permeability in vacuum, B is the magnetic field, r is the radial direction, z is the deformation direction and t is the time. Magnetic field changes vs. time are similar to changes of electric current in the work piece.

Fig. 1 represents the RLC circuit. The left circuit is the coil circuit and right one is the work piece. The sheet deformation is disregarded in non-coupling method and the differential equation can be written as [12]

$$L_c\frac{d}{dt}i_c(t)+R_c.i_c(t)+\frac{1}{C_c}\int_0^t i_t(t)dt=0 \qquad (2)$$

with initial conditions as

$$i_c(0)=0,[L_c\frac{d}{dt}i_c(t)]_{t=0}=V_\circ$$

where L_c is the overall inductance, R_c is the electrical resistance of the system, C_c is the total capacity, $i_c(t)$ is coil current and $V_\circ$ is the initial discharge voltage. The solution of equation (2) yields [13]

$$i(t)=\frac{V_\circ}{\omega L_c}e^{-\delta t}\sin(\omega t) \qquad (3)$$

where

$$\omega=\sqrt{\frac{1}{L_cC_c}-(\frac{R_c}{2L_c})^2} \qquad (4)$$

ω is angular frequency and δ is current damping coefficient. According to equation (3), the electric current vs. time is damped in sinusoidal form. The damping and circuit frequency is dependent on the parameters of RLC circuits.

The magnetic pressure distribution in the radial direction can be found analytically. Xu and colleagues provided the following equation for the Lorentz force originated from the spiral coil on the flat sheet

[DOI: 10.22068/ijmse.13.2.1]

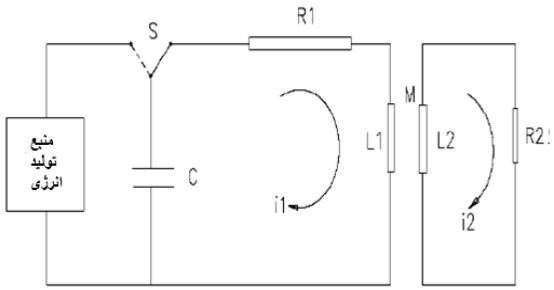

Fig. 1. Electrical model of the process.

$$f_z = -\mu\left(\frac{\eta N I_{max}}{2\pi h}\right)^2 \sqrt{(\alpha\beta)^2 + \left(\frac{\alpha}{\beta}\right)^2} * e^{2(\alpha\beta z - \delta t)} \sin(\omega t + \sin(\omega t + \frac{\alpha}{\beta} z + \theta) \sin\sin(\omega t + \frac{\alpha}{\beta} z) R^2(r) \quad (5)$$

$$\theta = \tan^{-1}(\frac{1}{\beta^2}) \quad (6)$$

where

$$\beta = \sqrt{\sqrt{\left(\frac{\psi(r) - \delta\mu\sigma}{\omega\mu\sigma}\right)^2 + 1} + \left(\frac{\psi(r) - \delta\mu\sigma}{\omega\mu\sigma}\right)} \quad (7)$$

$$\alpha = \sqrt{\frac{\omega\mu\alpha}{2}} \quad (8)$$

$$\psi(r) = -\frac{1}{R(r)}\left[\frac{\partial^2 R(r)}{\partial r^2} + \frac{1}{r}\frac{R(r)}{\partial r} - \frac{1}{r^2} R(r)\right] \quad (9)$$

$$R(r) = R_r(r) - R_f(r) \quad (10)$$

$$R_r(r) = (l_2 - r)\ln\left[\frac{(l_2 - r)^2 + h_2^2}{(l_2 - r)^2 + h_1^2}\right] + 2h_2 \tan^{-1}\left(\frac{l_2 - r}{h_2}\right) - 2h_1 \tan^{-1}\left(\frac{l_2 - r}{h_1}\right) - (l_1 - r)\ln\left[\frac{(l_1 - r)^2 + h_2^2}{(l_1 - r)^2 + h_1^2}\right] - 2h_2 \tan^{-1}\left(\frac{l_1 - r}{h_2}\right) + 2h_1 \tan^{-1}\left(\frac{l_1 - r}{h_1}\right) \quad (11)$$

$$R_f(r) = (l_2 + r)\ln\left[\frac{(l_2 + r)^2 + h_2^2}{(l_2 + r)^2 + h_1^2}\right] + 2h_2 \tan^{-1}\left(\frac{l_2 + r}{h_2}\right) - 2h_1 \tan^{-1}\left(\frac{l_2 + r}{h_1}\right) - (l_1 + r)\ln\left[\frac{(l_1 + r)^2 + h_2^2}{(l_1 + r)^2 + h_1^2}\right] - 2h_2 \tan^{-1}\left(\frac{l_1 + r}{h_2}\right) + 2h_1 \tan^{-1}\left(\frac{l_1 + r}{h_1}\right) \quad (12)$$

in which is the Lorentz force, R(r), R(f), ψ(r), α, β and θ are auxiliary functions, δ is damping of discharge circuit, t is time, ω is angular frequency, μ is magnetic permeability coefficient, I_{max} is maximum of the electric current, N is number of coil turns, r is radius, l_2 is outer radius of the coil, l_1 is coil inner radius, h, h_1 and h_2 are parameters related to the coil height and distance of the coil from sheet as displayed in

Fig. 2, σ is electrical conductivity, η is coefficient of error compensation for assuming the superconducting of the material and z is parameter of the thickness of the sheet depth.

Both damping and deformation reduce the magnetic pressure effects of the process. In non-coupling solution, the effects of sheet

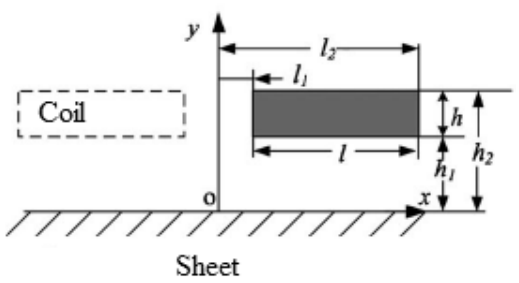

Fig. 2. Schematic figure of the coil and circular sheet [10].

[DOI: 10.22068/ijmse.13.2.1]

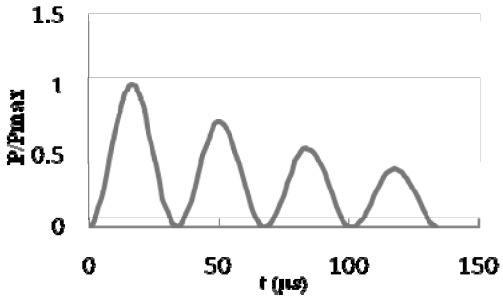

Fig. 3. Variation of pressure with time.

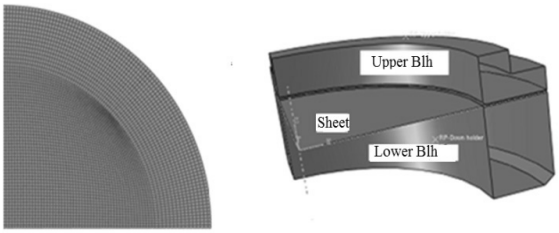

a b

Fig. 4. a) A quarter of the sheet in mesh mode, **b)** Electromagnetic sheet free forming assembely.

deformation are neglected in calculating the magnetic pressure and the magnitude of error in the calculations would be huge. Hashimoto et al. [12] stated that only the first cycle of the sinusoidal magnetic pressure is important.

Fig. 3 shows the magnetic pressure vs. time which damps with electrical current [5]. Duration of the first cycle is 67 μs and it is considered as a factor which exerts the magnetic pressure in the modeling.

3. THE MECHANICAL PART OF THE PROCESS

This part of the forming process is analyzed using FEM by Abaqus software. The obtained magnetic pressure by solving the electromagnetic sector is considered here as the input of mechanical part. Aluminum alloy 1050 sheet are used in this study and sheet characters are given in Table 1.

Fig. 4-a shows a quarter of the sheet which has been meshed with S4R elements and the type of mesh is structural. The sheet placed between the two holders and the assembled shape for a quarter of the sheet is shown in Fig. 4-b.

Table 1. Sheet characteristics used in this research.

Material	AAl 1050	Density	2750 kg/m^3
Young's modoul	80.7 GPa	Poisson ratio	0.33
Sheet diameter	110 mm	Bulged diameter	80 mm
Sheet thickness	0.5 mm		

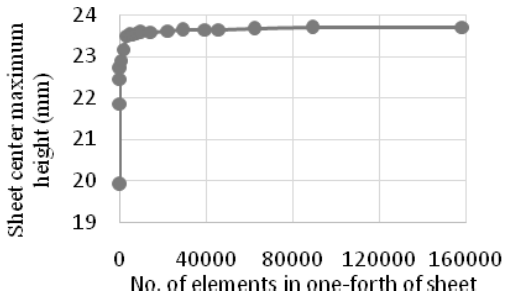

Fig. 5. Mesh sensitivity diagram.

Fig. 5 shows the mesh sensitivity diagram. Using 39600 elements, the amount of deformation of the center is 25.36 mm which is 0.5 mm less than that of the 160,000 elements which shows about 0.2% difference in the results. Then to reduce the computation time 39600 elements are considered.

4. MATERIAL HARDENING

Electromagnetic forming is a high speed forming process and the speed of electromagnetic sheet forming process is so high that it impacts the material hardening. In this study, both rate dependent and independent hardenings analyses have been used. For the hardening of AAl1050 sheet, Fenton and Daehn used the simplified

[DOI: 10.22068/ijmse.13.2.1]

model of Steinberg's [14]. In this model, the effect of strain rate on the hardening is ignored. Equation (13) is strain rate model used by Steinberg [14]

$$\sigma = 93(1+125\varepsilon^{p})^{0.1} \quad (13)$$

Correia et. al [9] used Holomon's strain rate dependent power law as

$$\sigma = \sigma_{\circ}(\varepsilon^{p})^{n} D(\dot{\varepsilon}^{p})^{m} \quad (14)$$

where $\sigma_{\circ}$ =118 MPa, D = 1.7 , n = 0.27 and m = 0.075 's. In equations (13) and (14), σ is effective stress, ε^{p} is effective plastic strain and $\dot{\varepsilon}^{p}$ is effective plastic strain rate.

In Fig. 6 the final geometry of the sheet obtained by applying two different hardening models and experimental results of Ref. [5] are compared. Strain rate dependent model provides more accurate results. The obtained results show the effect of sheet strain rate.

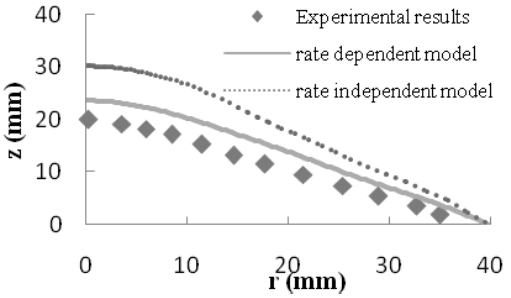

Fig. 6. Comparison of final geometry obtained from different hardening models.

5. EMF OF SHEET ON THE PUNCH

Aluminum alloy 1050 with a diameter of 80 mm and thickness of 0.5 mm is used to form the sheet on the punch. The Hollomon's strain rate dependent model is used for hardening. The spherical punch has a radius of 40 mm which is equal to the radius of the sheet. Position of the sheet is under the punch so that the tip of the punch is in contact with the sheet,

The coils mentioned in the literature do not yield acceptable results for sheet forming on the punch. Therefore, new coils with new design have been introduced by using analytical solution and by exerting the magnetic pressure produced by each coil on the sheet, results have been evaluated.

The coil with the maximum pressure of 9.5 MPa and other specifications are presented in Table 2 yielded the best results for forming of sheet on the punch. The magnetic pressure distribution on the sheet is shown in Fig. 8. The distortion of the sheet after the forming process and the normal distance between the sheet and the punch are two parameters which are studied here to evaluate the quality of forming. Three factors can be the cause of the gap between the sheet and the punch surface. The first one is the springback which happens because of elastic strains. The second one is using of smaller magnetic field than the required minimum amount to form the sheet and the third factor is the sheet return after hitting the punch surface which is because of using larger magnetic field than the required one.

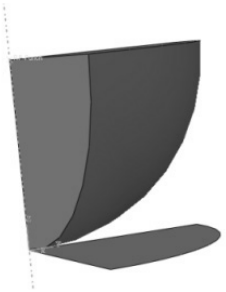

Fig. 7. Assembled punch and sheet in EMF.

Table 2. The parameters of the optimal coil to form the sheet on the punch.

Material	Copper	Inner radius	28 mm
No. of turns	6	Outer radius	40 mm
Pitch	2 mm	Conductivity	36 MS/m

[DOI: 10.22068/ijmse.13.2.1]

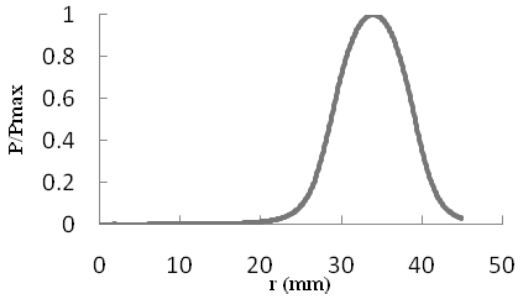

Fig. 8. The pressure distribution on the sheet produced by a coil with characteristics in Table 2.

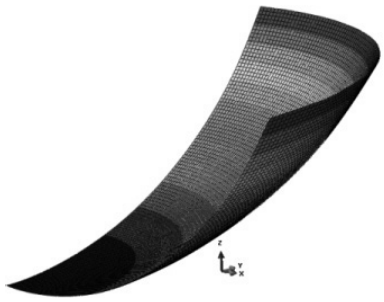

Fig. 9. The formed sheet on the punch.

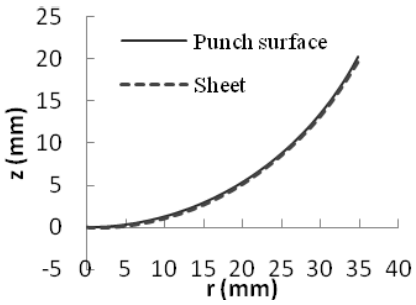

Fig. 10. Final geometry of the sheet on the punch.

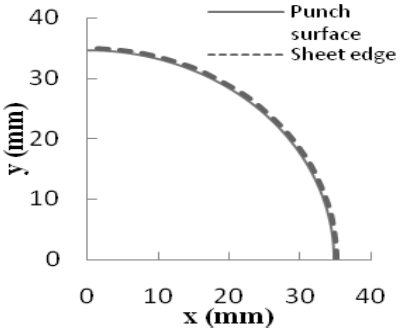

Fig. 11. Final position of the sheet edge on the punch surface.

Fig. 9 displays the formed sheet on the punch and Fig. 10 and Fig. 11 show the final sheet position in the radial and circumferential directions, respectively. It is seen that the sheet has been correctly formed on the punch.

Deformation history of forming of sheet on the punch is shown in Fig. 12. Pressure is applied to the plate until 67 μs and during this time the maximum height of sheet reaches 5 mm which is only about 20% of the final height. Inertia force completes the rest of the process which shows its decisive role here.

In case of improper pressure distribution, the sheet edge may lay back on itself. The coil used in [5] which correctly formed the sheet in free forming, is not proper to correctly form the sheet in forming on the punch and causes the edge movement in opposite direction. Applying the maximum pressure of 20 MPa, making the sheet as obtained in Fig. 13. In this figure, sheet position is shown in different time periods of the process. It is seen that the sheet does not place on the punch at the end of the process.

Fig. 14 shows the variation of thickness along the radius. It is seen that the amount of 96% of the initial thickness is the minimum thickness which occurs near the center of the plate. Sheet thickness increases gradually from the center towards the edge and on the edge the thickness increases by 0.01 mm.

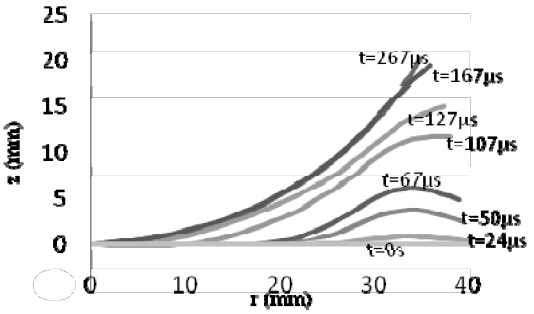

Fig. 12. Deformation history of sheet on the punch.

[DOI: 10.22068/ijmse.13.2.1]

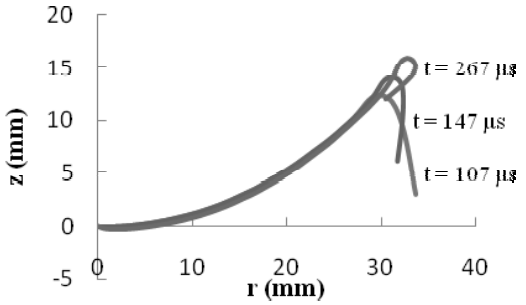

Fig. 13. The obtained sheet edge because of using improper pressure distribution.

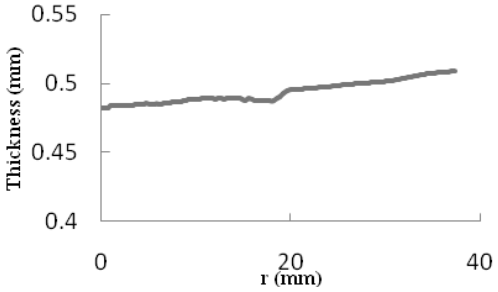

Fig. 14. Thickness variation along the radius.

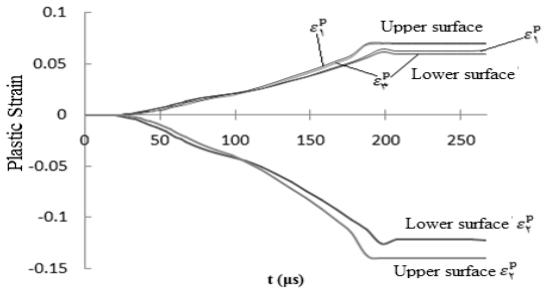

Fig. 15. Components of plastic strain versus time.

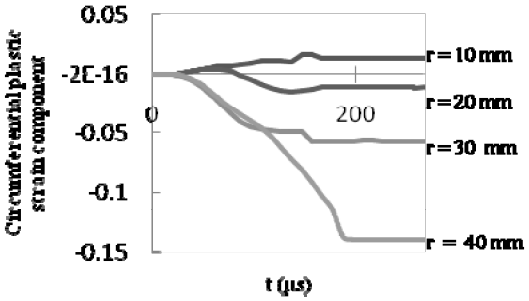

Fig. 16. Circumferential plastic strain versus time in different radii.

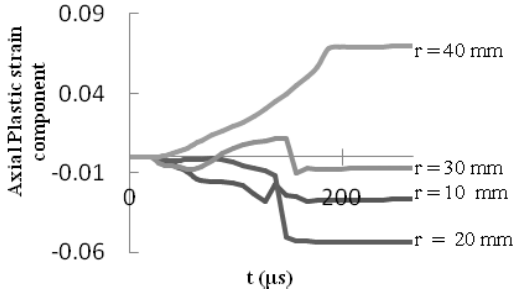

Fig. 17. Plastic strain in thickness direction component versus time in different radii.

Variations of plastic strain versus time for two points on the upper and lower surfaces of sheet are shown in

Fig. 15. In this figure, , and are in the radial, circumferential and thickness plastic strain components, respectively. and are almost equal. The radial component of the plastic strain is positive for all radii; however, the axial and circumferential components are positive in some radius and negative in some others, Figs. 16-17. Near the center, the is positive and is negative. In other words, the sheet is stretched in two directions in near-the-center spot causing a decrease in sheet thickness.

Fig. 17 shows that is positive and the thickness increases near the edge.

6. EMF OF SHEET INTO A SPHERICAL DIE

The main objective of this study is to achieve a final larger depth of workpiece by on-the-punch sheet forming instead of forming sheet into a die. In order to compare the obtained depths in the processes, a parameter called ratio of depth to diameter is defined. Risch succeeded in forming sheet inside a spherical mold with a depth to diameter ratio of 0.066 [6]. In the current research, the depth to diameter ratio of AA1050

[DOI: 10.22068/ijmse.13.2.1]

Table 3. The parameters of the optimal coil to form the sheet into the die.

Material	Copper	Inner radius	25 mm
No. of turns	5	Outer radius	37 mm
Pitch	2.5 mm	Conductivity	36 MS/m

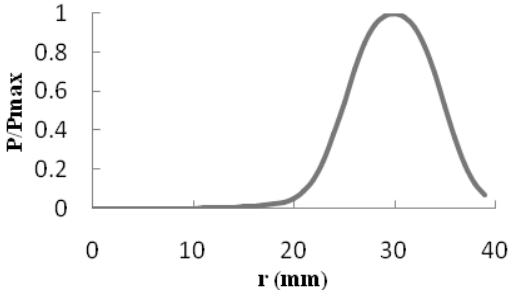

Fig. 18. The pressure distribution on the sheet produced by a coil with characteristics of Table 3.

with a thickness of 0.5 mm is studied and a maximum of 0.11 mm depth to diameter ratio is obtained. The maximum error value between the ideal geometry and the final geometry is 0.5 mm, this values is 3.5% of die height. For each depth to diameter ratio, special coil design is required. For forming sheet into the die with a depth to diameter ratio of 0.11, the die, which is a sector of a sphere, should have a diameter of 128 mm and a height of 14 mm. For forming sheet into the die, a coil with specifications presented in Table 3 and the pressure distribution indicated in

Fig. 18 provides the best results. The optimized maximum pressure for forming sheet into the die is 15.5 MP. By applying this pressure, the final shape of the sheet is obtained as Fig. 19 displays.

After whole investigation having been completed, the maximum achievable depth to diameter ratio in forming into the die was obtained as 0.11. For this ratio of depth to diameter, the height of the die is 14 mm which is a sector of the sphere with a diameter of 128 mm. On the other hand, the sheet was formed on a

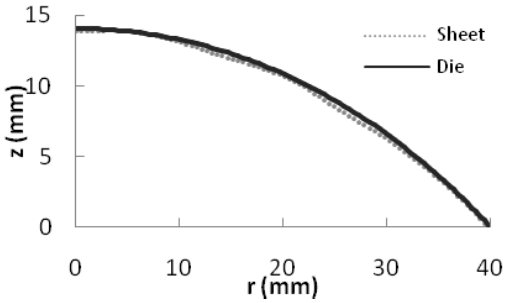

Fig. 19. Final shape of sheet into the die with the depth to diameter ratio of 0.11.

spherical punch whose diameter was 80 mm and the ultimate depth of the sheet was obtained as 20 mm. Depth to diameter ratio of 0.25 is obtained in the forming on the punch which is 227% more than that of forming in the die. In forming on the punch despite the more-than-twice increase of the depth to diameter ratio, the maximum tolerance between the sheet and the punch is 0.28 mm with the average tolerance 0.17 mm. These parameters for the ratio of 0.11 are 0.46 mm and 0.22, respectively. The results show that in spite of the greater ratio of depth to parameter, forming on the punch brings about better results.

7. CONCLUSIONS

1. In this study, it was shown that through considering true and valid assumptions, e.g., utilizing a proper duration time of magnetic pressure, the no-coupling method yields acceptable results.
2. Through considering the results drawn from rate dependent hardening model and rate-independent hardening model, it was revealed that in sheet EMF of aluminium, the speed of sheet deformation is so large for the strain-rate which influences on the mechanical behaviour of the material.
3. Using of sheet on a convex punch instead of sheet into a concave die, increases the forming depth considerably.

[DOI: 10.22068/ijmse.13.2.1]

REFERENCES

1. Kapitza, P. L., "A method for producing strong magnetic fields", Proceedings of the Royal Society Serine A, 1924, 105, 691–710.
2. Harvey, GW. and Brower, DF., Metal forming device and method, US Patent, 1958, No. 2976907.
3. Gobl, N., "Elektromagnetische umformversuche mit flachspulen", In DrittesKolloquium uber Grundlagen der elektrischen Hochgeschwindigkeitsbearbeitung, Berlin, 1969 , 78–94.
4. Al-Hassani, S. T. S., "Magnetic pressure distributions in sheet metal forming", Proceedings of the Conference on Electrical Methods of Machining, Forming and Coating, London, 1975, 1–10.
5. Takatsu, N., Kato, M., Sato, K. and Tobe, T., "High speed forming of metal sheets by electromagnetic force", Japan Society of Mechanical Engineers International Journal , 1988, 31(1), 142-148.
6. Risch, D., Beerwald, C., Brosius, A. and Kleiner, M., "On the significance of the die design for the electromagnetic sheet metal forming", Proceedings of the First International Conference on High speed Forming, Dortmund, 2004, 191–200.
7. Oliveira, D. A., Worswick, M. J., Finn, M. and Newman, D., "Electromagnetic forming of aluminium alloy sheet: free-form and cavity fill experiments and model", Journal of Materials Processing Technology, 2005, 170, 350–362.
8. Neugebauer, R., Loschmann, F., Putz, M., Koch, T. and Laux, G., "A production oriented approach in electromagnetic forming of metal sheets" Proceedings of the Second International Conference on High Speed Forming, Dortmund, 2006, 129–139.
9. Correia, J. P. M., Siddiqui, M. A., Ahzi, S., Belouettar, S. and Davies, R., "A simple model to simulate electromagnetic sheet free bulging process", International Journal of Mechanical Sciences, 2008, 50 1466–1475.
10. Xu, D., Liu, X., Fang, K. and Fang, H., "Calculation of electromagnetic force in electromagnetic forming process of metal sheet", Journal of Applied Physics, 2010, 107, 124907.
11. Xiao-Hui, C., Jian-Hua, M. and Ying, Z., "3D modelling and deformation analysis for electromagnetic sheet forming process", Transactions of Nonferrous Metals Society of China, 2012, 164-169.
12. Hashimoto, Y., Hideki, H., Miki, S. and Hideaki, N., "Local deformation and buckling of a cylindrical Al tube under magnetic impulsive pressure", Journal of Materials Processing Technology, 1999, 85, 209-212.
13. Serway, R. A., "Physics for scientists and engineers with modern physics", Third Edition, Saunders College Publishing, Toronto, 1990.
14. Fenton, G. K. and Daehn, G. S., "Modelling of electromagnetically formed sheet metal", Journal of Materials Processing Technology, 1998, 75, 6-16.

[DOI: 10.22068/ijmse.13.2.1]